



Received: 2025.12.13

Accepted: 2026.03.18

Available online: 2026.04.10

Published: 2026.XX.XX

Patterns of miRNA Expression in Primary and Metastatic Wilms Tumor

Authors' Contribution:
 Study Design A
 Data Collection B
 Statistical Analysis C
 Data Interpretation D
 Manuscript Preparation E
 Literature Search F
 Funds Collection G

ABCDEF 1 **Ádám Csók**
 AE 2 **Tamás Micsik**
 E 3 **Zsófia Magyar**
 E 4 **Tamás Tornóczy**
 E 2,5,6 **Levente Kuthi**
 BE 1 **Alexandra Barbara Kabai**
 E 1 **Krisztina Szirák**
 E 1 **Melinda Szilágyi**
 E 7 **Monika Csóka**
 E 8 **Gábor Ottóffy**
 E 1 **Beáta Soltész**
 E 1 **István Balogh**
 ABDEF 1 **Gergely Buglyó**

1 Department of Medical Genetics, Faculty of Medicine, University of Debrecen, Debrecen, Hungary
 2 Department of Pathology and Experimental Cancer Research, Semmelweis University, Budapest, Hungary
 3 Department of Obstetrics and Gynaecology, Baross Street Division, Semmelweis University, Budapest, Hungary
 4 Department of Pathology, University of Pécs Medical School and Clinical Center, Pécs, Hungary
 5 Department of Surgical and Molecular Pathology, Tumor Pathology Center, National Institute of Oncology, Budapest, Hungary
 6 HUN-REN-ONKOL-TTK-HCEMM Oncogenomics Research Group, National Institute of Oncology, Budapest, Hungary
 7 Department of Pediatrics, Semmelweis University, Budapest, Hungary
 8 Department of Pediatrics, University of Pécs Medical School and Clinical Center, Pécs, Hungary

Corresponding Author: Gergely Buglyó, e-mail: buglyo.gergely@med.unideb.hu

Financial support: None declared

Conflict of interest: None declared

Background: Wilms tumor (WT) development and the ability to form distant metastases are thought to be governed by a wide range of molecular factors, with prominent involvement of microRNAs (miRNAs). However, very few studies have explored alterations in miRNA expression between primary and metastatic WT, and all of them focused on a narrow set of miRNAs.

Material/Methods: We investigated miRNA expression in primary (10) and metastatic WT (6) and in healthy kidney specimens (10) using formalin-fixed, paraffin-embedded (FFPE) samples. miRNA was extracted from FFPE samples using miRNeasy FFPE Kits by Qiagen. Following reverse transcription, cDNA was amplified using miRCURY LNA miRNA Focus PCR Panels by Qiagen, which included primers against 84 specific miRNA targets, of which 81 were successfully amplified. Expression in metastatic WT was compared with primary tumors and healthy kidney tissue.

Results: Differential expression was particularly evident for 5 miRNAs (miR-17-3p, miR-34b-3p, miR-34c-5p, miR-375-3p, miR-616-3p). Our findings regarding the miR-34 family seem noteworthy in light of the limited existing literature, which similarly reports elevated expression of these miRNAs in WT, although they are more commonly downregulated in many other cancer types.

Conclusions: While the sample size in this study was modest, our findings suggest that metastatic tumors exhibit distinct miRNA expression patterns, which may have value for identifying tumors at risk of metastasis. We encourage further studies to validate or refute the role of the miRNAs proposed here in the development of metastasis.

Keywords: **Gene Expression Regulation, Neoplastic • Metastasis • MicroRNAs • Oncology • Polymerase Chain Reaction • Wilms Tumor**

Full-text PDF: <https://www.medscimonit.com/abstract/index/idArt/952424>

3473

5

5

37



Publisher's note: All claims expressed in this article are solely those of the authors and do not necessarily represent those of their affiliated organizations, or those of the publisher, the editors and the reviewers. Any product that may be evaluated in this article, or claim that may be made by its manufacturer, is not guaranteed or endorsed by the publisher

Introduction

Wilms Tumor Progression and Prognosis

Wilms tumor (WT; nephroblastoma) accounts for about 85% of pediatric renal tumors [1]. Molecular and histological similarities to the embryonic kidney are notable. Owing to a growing understanding of WT biology and improved treatment options, the 5-year survival rate now exceeds 90% in high-income countries. However, survival remains substantially lower in low- and middle-income regions (often below 50% in parts of Africa), where the incidence is among the highest worldwide [2].

In Europe, the International Society of Pediatric Oncology (SIOP) recommends preoperative chemotherapy followed by surgery, while an upfront nephrectomy is advocated in the United States by the Children's Oncology Group [3]. Only about 17% of WT cases metastasize, resulting in poorer outcomes [4]. Metastasis mainly occurs in WT with unfavorable histology. Blastemal and diffuse anaplastic WTs are classified as high-risk tumors according to SIOP and are often metastasized [5]. Anaplasia is defined by the presence of polypoid, atypical, mitotic figures, an enlargement in nuclear size, and hyperchromasia of the tumor cells [6]. Lung metastasis is the most common, accounting for about 80% of cases, while metastases to the liver, bone, brain, and lymph nodes are less frequently observed [7]. A better understanding of the molecular background of WT metastasis is essential for accurate risk assessment and follow-up.

Role of MicroRNA Expression in Metastasis Development

MicroRNAs (miRNAs) are a key class of messenger RNA (mRNA) regulators, implicated in primary and metastatic cancer [8], which undergo a multi-step maturation process. They mostly bind to the 3'-untranslated (3' UTR) region of targets to suppress their expression, but may also interact with other specific regions, including the 5' UTRs of mRNAs or the promoters and coding sequences of target genes [9]. In this study, our objective was to gain a better insight into the biological background of WT metastasis formation through the analysis of miRNA expression patterns. Promising results were obtained with several miRNAs.

Few papers can be found on the subject and none of them appear to have taken a broad approach, involving only a limited number of miRNAs [10,11]. (These findings are discussed below in the section "WT Metastases and Their miRNA Signatures.") To our knowledge, our paper is the first to report expression differences across a relatively wide range of miRNAs (84 studied in total, out of which 81 were successfully amplified) between primary and metastatic WTs, although the modest sample size, particularly for metastatic samples (n=6), constrains statistical power and positions the findings as exploratory.

Material and Methods

Patients

In cooperation with the departments of pathology of 3 Hungarian universities (Semmelweis University, University of Szeged, and University of Pécs), formalin-fixed, paraffin-embedded (FFPE) samples were collected from primary WTs (10), metastatic tumors (6), and healthy kidney tissue obtained from unaffected areas of WT and nephroblastomatosis surgical specimens (10). Overall, 12 patients were included in our study, and in 6 cases we obtained multiple samples. One patient contributed 2 metastatic samples (1 from each lung), while in another patient, 3 histologically different samples, 1 metastatic, and 2 primary tumor samples (1 with stromal and 1 with mixed histology) were studied and compared (Table 1). The 10 primary WT samples were selected on the basis of their frequency of occurrence and metastasis production (4 regressive, 3 mixed, 2 blastemal, and 1 stromal).

In accordance with the SIOP protocol, preoperative chemotherapy was administered using a regimen based on vincristine and actinomycin D, while those presenting with metastatic disease (stage IV) received a more intensive regimen including doxorubicin [4].

RNA Extraction and Reverse Transcription

We followed laboratory protocols as previously published by us and others [12-15]. Here, miRNA extraction was performed using miRNeasy FFPE Kits by Qiagen (Hilden, Germany). After the extraction, RNA concentration was measured by NanoDrop (Thermo Scientific NanoDrop Lite). Concentrations lower than 50 ng/ μ L were considered inadequate; otherwise, the step was followed by reverse transcription (RT) using miRCURY LNA RT Kits (Qiagen). Instead of 20 ng, as recommended by the manufacturer's protocol, 200 ng RNA template was included per reaction mix to account for degraded RNA molecules in the size range of miRNA that are detectable in FFPE samples [16]. Total reaction volumes were 20 μ L for each polymerase chain reaction (PCR) assay. Finally, cDNA was stored at -20°C until a RT-qPCR was performed.

Analyzing miRNA Expression Levels with RT-qPCR Arrays

RT-qPCR experiments were performed using miRCURY LNA miRNA Focus PCR Panels (Qiagen) and miRCURY LNA SYBR Green PCR Kits (Qiagen). On the PCR array, 84 individual primer pairs against specific miRNA targets were located in separate wells. These miRNAs are known to play various roles in WTs and in other genitourinary tumors [15]. Primers for small nucleolar RNA, C/D box 44 (SNORD44), small nucleolar RNA, C/D box 38B (SNORD38B), small nucleolar RNA, C/D box 49A

Table 1. Patients with primary and/or with metastatic tumors were included in the study. From 2 patients, primary and metastatic samples were included, while from 3 patients, only metastatic samples were processed. (*) Denotes patients who contributed multiple samples. For patients 1, 2, and 3, control samples from tumor-free regions of the kidney (C1-C3, respectively) were analyzed in addition to the primary tumor samples. Patient 5 contributed a primary tumor and a metastatic sample. Patient 9 contributed metastatic samples from both lungs collected at different time points. In patient 12, two primary Wilms tumor (WT) samples with different histological types (stromal and mixed) were analyzed in addition to the metastatic sample.

Patient ID	Age at surgery	Sex	Laterality of primary WT	Histology of primary WT	Metastasis
*1	3 Years	Female	Left	Blastemal	–
*2	2 Years	Male	Left	Mixed	–
*3	8 Years	Male	Right	Blastemal	–
4	3 Years	Female	Right	Regressive	–
*5	5 Years	Male	Right	Regressive	Lung (unilateral)
6	2 Years	Female	Right	Regressive	–
7	5 Months	Female	Right	Mixed	–
8	4 Years	Male	Left	Regressive	–
*9	4 Years	Male		–	Lungs (bilateral)
10	3 Years	Male		–	Lung (unilateral)
11	11 Years	Female		–	Lung (unilateral)
*12	2 Years	Female	Left	Mixed; stromal	Lung (unilateral)

(SNORD49A), and U6 small nuclear RNA (U6 snRNA) were also present in the arrays as endogenous controls. Technical replicates were not performed, due to the limited availability of metastatic WT samples and financial constraints associated with the array platform.

Complementary DNAs from control, primary, and metastatic samples were amplified with a Roche LightCycler 96 PCR system (Roche, Basel, Switzerland). The total reaction volume (20 µL) from the RT was used for the experiment. PCR steps included a 2-min heat activation at 95°C followed by a 2-step cycling consisting of a denaturation for 10 s at 95°C and a combined annealing/extension for 60 s at 56°C. The experiment was continued for 45 cycles. Finally, a melting curve analysis (95°C for 60 seconds, 40°C for 60 seconds, then 65°C to 97°C with a ramp of 0.07°C/second) was performed. Cycle threshold (Ct) values over 40 (in all cases) and those between 35 and 40 (in case of a dubious melting curve) were considered negative (unamplified). Data were evaluated with the LightCycler 96 software (Roche, version 1.1).

ΔCt (delta Ct) values were calculated relative to control Ct values defined as the mean of the 4 endogenous controls included in the PCR arrays by the manufacturer, shown to be stable in

the tissue context in our previous work [15]. ΔCt values were determined separately in healthy tissue, primary WT, and metastatic samples for each miRNA, and compared using statistical methods as described below.

Network Analysis

A network analysis was performed for the targets of 5 miRNAs (miR-17-3p, miR-34b-3p, miR-375-3p, miR-616-3p, and miR-34c-5p) using the miRNet web tool (<https://www.mirnet.ca/>), which integrates predicted and experimentally validated interactions. Results were obtained for all 5 miRNAs except miR-375-3p, for which no interactions were identified; therefore, it was not included in the final network. Network analysis was followed by a functional gene enrichment analysis (KEGG pathways and Reactome database).

The miRNet platform was used for network construction and functional enrichment analysis using its default parameters. Pathway enrichment analysis in miRNet is performed using multiple-testing correction based on the Benjamini-Hochberg false discovery rate. The background gene sets correspond to the genes annotated in the selected pathway databases (Reactome and KEGG) within the miRNet framework.

Table 2. Delta cycle threshold (ΔCt) values for 10 primary Wilms tumor (WT) samples (from 9 patients). The rightmost column shows permutation analysis results: for each miRNA, absolute ΔCt differences were calculated for all sample pairs, and the *P* value represents the probability that a random pair has a ΔCt difference \leq that between the 2 samples from patient 12.

miRNA	Patient 1	Patient 2	Patient 3	Patient 4	Patient 5	Patient 6	Patient 7	Patient 8	Patient 12 (stromal)	Patient 12 (mixed)	Mean	Permutation <i>P</i> value
hsa-let-7a-5p	-1.33	-0.27	-2.26	-0.74	-0.12	-2.94	-0.12	1.18	-2.08	-0.64	-0.93	0.53
hsa-let-7b-5p	-0.86	0.65	-1.34	0.33	-0.27	-2.96	0.55	1.53	-2.18	-0.46	-0.50	0.60
hsa-let-7c-5p	0.51	0.21	-0.92	-0.45	0.58	-1.03	0.30	2.15	-1.43	0.16	0.01	0.71
hsa-let-7f-5p	1.26	2.34	1.36	2.44	3.35	-0.6	2.27	3.93	1.39	3.14	2.09	0.62
hsa-miR-100-5p	1.17	1.72	2.27	1.00	1.86	-1.2	1.65	2.88	0.59	2	1.39	0.71
hsa-miR-101-3p	2.55	5.20	3.83	6.52	5.45	1.84	5.48	5.75	4.09	5.9	4.66	0.60
hsa-miR-106b-5p	1.69	3.17	0.32	4.89	5.02	-0.66	1.73	4.75	3.21	3.66	2.78	0.11
hsa-miR-125a-5p	-2.75	-0.80	-2.74	-0.32	-0.14	-2.77	-0.43	1.22	-1.02	0.27	-0.95	0.42
hsa-miR-125b-5p	-2.10	-2.43	-0.17	-2.82	-2.03	-4.77	-2.08	-0.75	-3.73	-2.11	-2.30	0.58
hsa-miR-126-3p	-0.31	1.47	1.45	2.38	1.67	0.29	2.25	2.67	1.27	3.06	1.62	0.62
hsa-miR-126-5p	4.02	5.56	0.35	6.29	5.26	3.28	6.10	6.30	5.02	7.33	4.95	0.69
hsa-miR-128-3p	6.27	3.70	6.44	7.47	8.22	3.94	5.26	9.55	2.88	3.83	5.75	0.24
hsa-miR-133a-3p	6.83	-1.32	7.23	5.65	3.27	3.37	2.77	7.60	-2.36	-0.15	3.29	0.62
hsa-miR-135a-5p	3.06	4.57	0.39	6.55	8.59	1.07	4.15	7.83	6.69	5.45	4.83	0.20
hsa-miR-135b-5p	2.96	4.75	0.09	7.57	9.16	2.21	5.36	8.28	8.22	5.18	5.38	0.76
hsa-miR-141-3p	7.04	3.99	–	6.85	12.06	4.33	5.49	7.81	7.65	7.21	6.94	0.17
hsa-miR-143-3p	2.69	2.18	3.23	2.22	0.35	-0.88	2.54	3.15	1.39	3.2	2.01	0.64
hsa-miR-145-5p	-1.81	0.01	-0.81	-1.56	-3.10	-2.18	0.57	0.68	-1.18	0.87	-0.85	0.67
hsa-miR-146a-5p	4.99	5.35	3.92	3.99	5.47	3.71	6.85	6.40	5.34	6.5	5.25	0.44
hsa-miR-146b-5p	1.28	3.45	-0.08	3.84	4.57	0.94	3.86	4.83	3.82	5.07	3.16	0.40
hsa-miR-148a-3p	5.57	5.16	5.87	4.88	5.20	1.53	5.37	6.36	2.72	4.98	4.76	0.69
hsa-miR-15a-5p	3.41	2.48	1.99	2.78	3.25	-0.24	3.14	3.86	2.60	3.61	2.69	0.31
hsa-miR-15b-5p	5.94	5.75	1.77	3.95	5.72	1.07	4.49	6.06	3.89	5.25	4.39	0.49

APPROVED GALLEY PROOF

Table 2 continued. Delta cycle threshold (Δ Ct) values for 10 primary Wilms tumor (WT) samples (from 9 patients). The rightmost column shows permutation analysis results: for each miRNA, absolute Δ Ct differences were calculated for all sample pairs, and the *P* value represents the probability that a random pair has a Δ Ct difference \leq that between the 2 samples from patient 12.

miRNA	Patient 1	Patient 2	Patient 3	Patient 4	Patient 5	Patient 6	Patient 7	Patient 8	Patient 12 (stromal)	Patient 12 (mixed)	Mean	Permutation <i>P</i> value
hsa-miR-16-5p	-1.78	0.26	-1.51	-0.16	0.77	-3.08	0.66	1.00	-0.37	0.82	-0.34	0.47
hsa-miR-17-5p	0.53	3.04	0.74	4.23	4.74	-1.31	1.34	4.74	3.86	3.5	2.54	0.13
hsa-miR-17-3p	4.99	6.92	4.67	8.42	9.18	4.09	5.68	9.37	7.29	7.63	6.82	0.07
hsa-miR-181a-5p	-0.46	-0.34	-1.54	1.67	2.86	-3.17	-0.39	3.53	0.56	0.48	0.32	0.02
hsa-miR-181b-5p	1.90	2.21	-1.01	3.50	4.55	-0.77	0.96	5.48	2.52	2.43	2.18	0.02
hsa-miR-182-5p	5.08	6.48	3.83	8.89	10.09	2.6	5.27	10.67	6.41	5.73	6.50	0.16
hsa-miR-183-5p	6.78	6.63	2.38	9.27	10.86	3.04	5.80	11.40	6.06	6.35	6.86	0.07
hsa-miR-184	8.29	12.74	–	13.95	17.63	9.15	–	14.35	10.69	15.78	12.82	0.71
hsa-miR-194-5p	2.63	6.88	3.76	7.96	8.55	3.55	6.83	8.68	6.92	7.64	6.34	0.20
hsa-miR-195-5p	2.02	6.23	3.99	7.15	3.59	2.62	8.27	5.78	4.79	5.92	5.03	0.24
hsa-miR-196a-5p	1.06	7.65	-4.92	4.90	5.04	-1.12	1.59	6.36	3.21	5.54	2.93	0.67
hsa-miR-19b-3p	-0.72	2.35	0.90	4.15	4.23	-1.77	1.43	3.72	2.32	2.76	1.94	0.13
hsa-miR-200b-3p	4.30	2.85	4.65	5.31	10.98	2.99	4.27	6.46	5.99	4.35	5.21	0.47
hsa-miR-200c-3p	4.23	1.52	4.18	3.26	9.86	3.03	3.26	5.43	4.68	4.61	4.40	0.02
hsa-miR-203a-3p	10.72	8.39	–	13.46	13.29	8.69	11.58	11.08	10.37	10.83	10.93	0.17
hsa-miR-205-5p	–	3.84	–	8.06	10.61	6.8	6.27	6.18	9.00	6.72	7.18	0.50
hsa-miR-20a-5p	-0.44	1.91	-1.34	3.08	3.71	-2.16	0.27	3.52	2.78	2.45	1.38	0.09
hsa-miR-20b-5p	7.58	12.34	11.90	12.68	12.31	6.89	9.97	12.02	10.68	11.02	10.74	0.09
hsa-miR-21-5p	0.78	-0.83	-3.03	-1.38	-0.66	-2.19	0.76	-0.51	-1.19	0.02	-0.82	0.04
hsa-miR-218-5p	4.88	4.94	1.65	5.09	6.66	1.43	4.88	7.30	5.76	5.73	4.83	0.02
hsa-miR-22-3p	4.48	1.72	4.49	3.04	2.22	1.13	3.52	3.50	2.18	2.84	2.91	0.66
hsa-miR-221-3p	2.38	4.26	1.61	3.08	4.59	1.29	2.75	5.90	4.28	3.99	3.41	0.09
hsa-miR-222-3p	0.88	4.11	2.14	2.69	3.46	0.86	3.56	4.75	2.32	3.83	2.86	0.56

APPROVED GALLEY PROOF

Table 2 continued. Delta cycle threshold (ΔCt) values for 10 primary Wilms tumor (WT) samples (from 9 patients). The rightmost column shows permutation analysis results: for each miRNA, absolute ΔCt differences were calculated for all sample pairs, and the P value represents the probability that a random pair has a ΔCt difference \leq that between the 2 samples from patient 12.

miRNA	Patient 1	Patient 2	Patient 3	Patient 4	Patient 5	Patient 6	Patient 7	Patient 8	Patient 12 (stromal)	Patient 12 (mixed)	Mean	Permutation P value
hsa-miR-223-3p	2.59	3.38	3.66	3.04	3.78	0.84	3.51	4.11	3.45	4.68	3.30	0.49
hsa-miR-224-5p	7.64	9.30	6.57	6.96	8.51	6.62	9.21	9.38	7.66	8.63	8.05	0.33
hsa-miR-23b-3p	-2.54	0.61	-3.29	0.30	0.72	-1.06	1.78	2.33	0.15	1.16	0.01	0.38
hsa-miR-24-3p	-1.28	0.79	0.50	1.79	1.13	-1.27	1.76	2.48	-0.26	1.07	0.67	0.51
hsa-miR-25-3p	-0.79	2.28	-3.61	3.46	4.24	-1.01	1.27	4.51	2.62	3.01	1.60	0.09
hsa-miR-26a-5p	-1.40	0.79	-0.97	0.44	1.72	-1.71	1.49	2.25	0.26	1.89	0.47	0.60
hsa-miR-26b-5p	1.08	2.98	0.63	3.35	3.98	-0.08	3.52	4.42	2.30	3.96	2.61	0.62
hsa-miR-27a-3p	0.16	2.08	1.12	3.03	1.99	-0.12	2.65	3.33	0.96	2.46	1.76	0.58
hsa-miR-27b-3p	-0.93	1.48	-0.10	2.09	1.65	-0.49	2.20	3.13	0.71	1.97	1.17	0.47
hsa-miR-296-5p	5.15	7.29	5.39	7.53	6.54	5.85	5.71	8.19	6.55	6.43	6.46	0.12
hsa-miR-29b-3p	8.36	5.43	5.80	5.75	4.55	3.89	7.03	5.60	5.83	7.11	5.93	0.47
hsa-miR-30c-5p	-1.82	1.14	-1.43	2.40	2.93	-0.66	2.62	3.76	1.80	2.53	1.33	0.50
hsa-miR-31-5p	5.79	7.31	6.58	8.00	7.90	4.58	8.14	6.92	6.79	7.33	6.93	0.18
hsa-miR-32-5p	4.55	5.44	2.14	6.44	7.45	3.06	5.42	6.92	6.26	6.69	5.44	0.13
hsa-miR-330-3p	6.62	9.21	7.47	9.27	8.66	7.44	9.06	9.67	7.88	9.35	8.46	0.62
hsa-miR-331-3p	4.82	2.91	3.34	3.95	4.02	2.4	3.08	4.53	2.59	4.04	3.57	0.58
hsa-miR-34a-5p	5.55	3.42	5.90	4.76	4.20	3.07	6.02	5.18	2.30	3.23	4.36	0.31
hsa-miR-34b-3p	11.71	14.72	-	13.57	12.34	-	14.34	13.78	11.24	12.71	13.05	0.53
hsa-miR-34c-5p	-	13.10	-	13.75	13.15	9.74	-	13.17	9.79	12.82	12.22	0.57
hsa-miR-361-5p	0.35	3.28	0.94	2.85	3.82	-0.2	2.93	5.03	1.71	2.95	2.36	0.51
hsa-miR-365a-3p	5.61	4.42	5.45	4.86	4.09	3.39	5.41	6.35	3.80	4.81	4.82	0.36
hsa-miR-374b-5p	0.99	4.77	-0.54	4.09	4.98	1.38	3.98	5.60	3.62	4.9	3.38	0.51
hsa-miR-375-3p	10.17	7.89	9.00	11.36	-	6.45	11.65	12.99	7.72	9.82	9.67	0.47

APPROVED GALLEY PROOF

Table 2 continued. Delta cycle threshold (Δ Ct) values for 10 primary Wilms tumor (WT) samples (from 9 patients). The rightmost column shows permutation analysis results: for each miRNA, absolute Δ Ct differences were calculated for all sample pairs, and the *P* value represents the probability that a random pair has a Δ Ct difference \leq that between the 2 samples from patient 12.

miRNA	Patient 1	Patient 2	Patient 3	Patient 4	Patient 5	Patient 6	Patient 7	Patient 8	Patient 12 (stromal)	Patient 12 (mixed)	Mean	Permutation <i>P</i> value
hsa-miR-425-5p	3.78	4.45	2.95	5.21	5.38	1.53	3.88	5.96	4.34	5.28	4.27	0.31
hsa-miR-449a	–	11.58	–	–	–	–	13.02	–	12.78	14.13	12.88	0.67
hsa-miR-455-5p	7.16	5.61	5.92	8.04	8.93	4.38	6.91	8.33	5.07	7.08	6.74	0.62
hsa-miR-494-3p	9.62	7.41	–	8.59	9.03	6.28	7.90	10.34	5.53	8.04	8.08	0.78
hsa-miR-616-3p	11.21	14.22	–	14.18	12.81	–	13.08	15.31	13.17	17.54	13.94	0.89
hsa-miR-7-5p	10.96	8.64	6.07	10.19	11.77	5.53	7.68	10.39	10.62	10.53	9.24	0.02
hsa-miR-9-3p	11.78	–	–	12.59	11.64	6.5	13.74	13.94	14.44	13.27	12.24	0.46
hsa-miR-92a-3p	-1.78	-0.74	-3.71	0.00	0.51	-3.63	-1.09	0.94	-0.41	0.43	-0.95	0.29
hsa-miR-93-5p	0.37	2.39	-1.15	4.00	4.43	-0.88	0.92	4.71	3.41	3.02	2.12	0.11
hsa-miR-96-5p	7.98	6.69	6.56	10.40	11.29	3.36	6.12	11.46	7.53	6.41	7.78	0.40
hsa-miR-99a-5p	1.18	0.18	3.06	0.06	1.18	-0.68	1.01	2.61	-1.14	0.76	0.82	0.69
hsa-miR-99b-5p	-0.53	1.69	-1.25	1.90	2.57	-0.36	1.72	3.92	1.55	3.18	1.44	0.60
Median:												
0.47												

Statistical Analysis

Statistical analyses were performed using MedCalc software (version 23.0.9). We compared Δ Ct values derived from metastatic samples with the expression results of both the healthy samples and the primary WT samples by 2 separate *t* tests, followed by a Kruskal-Wallis test to compare all 3 groups. (Due to the relatively small sample size, formal assessments of normality and variance homogeneity have limited statistical power. Therefore, we evaluated results using parametric and nonparametric tests, and prioritized findings that consistently yielded low *P* values under both approaches.) As this study was designed as an exploratory, hypothesis-generating analysis rather than a confirmatory study with predefined endpoints, no fixed significance threshold was applied and multiple-testing corrections were not used as a decision criterion. Instead, exact *P* values are reported for all miRNAs to allow transparent interpretation of data.

Using the MedCalc software, log₂ fold change (log₂FC) values of distinct primary and metastatic samples from the same patients (patients 9 and 12; **Table 1**) were compared and visualized using multiple line graphs. To evaluate the potential impact of including multiple samples originating from the same patients, we assessed inpatient similarity using permutation analysis and performed parallel statistical analyses with and without 1 of the 2 same-patient metastatic samples. This approach was used to test the robustness of the observed miRNA expression differences to potential inpatient correlation (see “Inpatient Variability Between Primary and Metastatic WT Samples” in the Results).

Results

Alterations of miRNA Expression

While 81 miRNAs were successfully amplified in most samples (**Tables 2-4**), 3 out of the 84 that were present on the array

Table 3. Delta cycle threshold (Δ Ct) values for 6 metastatic Wilms tumor (WT) samples (from 5 patients). Logarithmic fold change (\log_2 FC) values between groups are shown in the right.

miRNA	Patient 5	Patient 9 (left lung met.)	Patient 9 (right lung met.)	Patient 10	Patient 11	Patient 12	Mean	\log_2 FC (metastatic to control)	\log_2 FC (metastatic to primary)
hsa-let-7a-5p	-2.76	0.25	2.14	-1.92	-0.85	-2.76	-0.98	0.03	0.05
hsa-let-7b-5p	-1.26	0.52	3.01	-1.02	0.15	-2.96	-0.26	-0.56	-0.24
hsa-let-7c-5p	-1.54	1.46	3.09	-1.73	-0.01	-1.33	-0.01	0.39	0.02
hsa-let-7f-5p	-1.39	3.15	5.05	-1.41	1.26	0.37	1.17	0.39	0.92
hsa-miR-100-5p	1.03	3.52	5.17	-0.34	2.00	-1	1.73	-0.17	-0.34
hsa-miR-101-3p	2.56	4.90	6.12	0.15	2.47	4.02	3.37	-0.20	1.29
hsa-miR-106b-5p	-0.74	3.60	2.72	-1.22	2.20	0.99	1.26	2.56	1.52
hsa-miR-125a-5p	-3.37	0.03	0.82	-3.23	-1.67	-3.29	-1.78	0.37	0.83
hsa-miR-125b-5p	-2.39	0.42	2.44	-3.05	-1.16	-5.17	-1.48	-0.69	-0.82
hsa-miR-126-3p	-0.65	-0.32	2.52	-3.92	-1.92	-0.77	-0.84	0.66	2.46
hsa-miR-126-5p	1.10	3.54	6.54	-0.39	2.25	2.51	2.59	1.19	2.36
hsa-miR-128-3p	4.31	7.42	6.67	4.43	6.18	5.1	5.68	1.58	0.07
hsa-miR-133a-3p	5.16	6.15	9.11	4.86	4.35	4.86	5.75	-0.30	-2.46
hsa-miR-135a-5p	-0.38	5.23	4.58	0.26	0.97	1.94	2.10	1.16	2.73
hsa-miR-135b-5p	-0.06	4.69	4.25	1.00	1.43	3.36	2.44	3.50	2.93
hsa-miR-141-3p	6.11	3.31	6.47	2.64	2.32	3.51	4.06	-0.92	2.88
hsa-miR-143-3p	0.76	2.36	4.29	0.30	0.56	1.72	1.67	-0.90	0.34
hsa-miR-145-5p	-2.00	-1.22	1.66	-3.13	-2.70	-0.8	-1.36	-0.51	0.51
hsa-miR-146a-5p	2.71	4.66	6.28	2.45	4.39	3.01	3.92	0.64	1.33
hsa-miR-146b-5p	-0.02	4.21	4.79	-1.59	1.75	1.37	1.75	2.16	1.41
hsa-miR-148a-3p	1.08	5.12	6.00	3.07	4.52	4.92	4.12	-0.29	0.65
hsa-miR-15a-5p	0.23	3.45	4.64	0.92	3.47	1.73	2.41	0.59	0.28
hsa-miR-15b-5p	0.26	5.19	5.55	1.18	2.40	4.26	3.14	2.04	1.25
hsa-miR-16-5p	-3.35	0.65	1.72	-5.59	-0.90	-2.28	-1.62	1.59	1.28
hsa-miR-17-5p	-1.60	2.98	1.55	-2.59	2.92	0.39	0.61	2.34	1.93
hsa-miR-17-3p	3.25	7.15	6.10	2.19	2.76	3.65	4.18	3.10	2.64
hsa-miR-181a-5p	-1.31	1.68	1.83	-2.04	0.73	-3.81	-0.49	1.59	0.80
hsa-miR-181b-5p	-0.28	3.96	3.85	-0.45	2.40	-1.86	1.27	2.11	0.91
hsa-miR-182-5p	0.26	7.88	7.08	1.32	7.17	0.5	4.03	4.72	2.47
hsa-miR-183-5p	0.68	8.31	7.64	2.24	5.14	1.57	4.26	4.88	2.59
hsa-miR-184	–	10.09	–	10.51	9.24	8.79	9.66	-1.86	3.16
hsa-miR-194-5p	2.84	6.90	7.00	0.42	5.39	4	4.42	-3.50	1.91
hsa-miR-195-5p	2.69	3.94	6.48	-0.56	3.23	3.83	3.27	-0.08	1.77

APPROVED GALLEY PROOF

Table 3 continued. Delta cycle threshold (Δ Ct) values for 6 metastatic Wilms tumor (WT) samples (from 5 patients). Logarithmic fold change (\log_2 FC) values between groups are shown in the right.

miRNA	Patient 5	Patient 9 (left lung met.)	Patient 9 (right lung met.)	Patient 10	Patient 11	Patient 12	Mean	\log_2 FC (metastatic to control)	\log_2 FC (metastatic to primary)
hsa-miR-196a-5p	-5.94	5.75	4.05	-4.42	-1.44	3.78	0.30	3.25	2.63
hsa-miR-19b-3p	-0.62	2.96	1.96	-3.53	-0.75	-0.18	-0.03	1.35	1.96
hsa-miR-200b-3p	4.92	4.33	7.50	2.77	3.30	1.87	4.11	-2.85	1.10
hsa-miR-200c-3p	2.40	0.93	4.51	0.10	0.36	0.78	1.51	-0.54	2.89
hsa-miR-203a-3p	8.17	6.00	9.76	6.09	5.37	6.56	6.99	-0.21	3.94
hsa-miR-205-5p	8.09	5.53	8.23	6.77	7.94	6.52	7.18	1.59	0.00
hsa-miR-20a-5p	-3.00	2.13	0.92	-3.43	2.03	-1.2	-0.42	2.03	1.80
hsa-miR-20b-5p	8.22	11.15	9.94	8.19	11.67	11.45	10.10	-0.23	0.64
hsa-miR-21-5p	-3.21	0.94	2.49	-4.36	-1.17	-1.58	-1.15	0.92	0.32
hsa-miR-218-5p	-2.21	5.68	4.89	-1.41	4.23	2.47	2.27	3.51	2.56
hsa-miR-22-3p	2.93	2.82	4.92	3.03	3.76	2.85	3.38	-1.52	-0.47
hsa-miR-221-3p	-1.29	3.92	4.14	2.87	0.63	1.14	1.90	1.65	1.51
hsa-miR-222-3p	-0.34	3.06	4.77	1.23	2.21	1.37	2.05	0.89	0.81
hsa-miR-223-3p	2.56	2.67	5.32	-2.25	1.08	1.95	1.89	1.62	1.42
hsa-miR-224-5p	4.89	8.68	10.15	5.57	5.70	5.97	6.83	1.75	1.22
hsa-miR-23b-3p	-4.91	0.94	1.61	-5.07	-0.86	-1.04	-1.55	1.30	1.57
hsa-miR-24-3p	-2.92	1.08	2.02	-3.77	-0.84	-0.23	-0.78	1.16	1.45
hsa-miR-25-3p	-4.02	2.73	2.40	-3.85	-1.86	-2.73	-1.22	4.00	2.82
hsa-miR-26a-5p	-2.06	1.40	2.64	-4.13	-0.48	-0.42	-0.51	0.24	0.98
hsa-miR-26b-5p	-0.45	3.31	4.74	-1.32	1.96	1.65	1.65	0.41	0.97
hsa-miR-27a-3p	-2.77	2.39	3.82	-3.27	0.41	0.88	0.24	0.96	1.52
hsa-miR-27b-3p	-3.61	1.98	2.84	-4.19	-0.12	0.06	-0.51	1.04	1.68
hsa-miR-296-5p	12.33	5.93	6.58	4.99	8.31	9.42	7.93	-1.81	-1.46
hsa-miR-29b-3p	4.61	3.74	6.42	4.96	6.24	6.82	5.46	-1.56	0.47
hsa-miR-30c-5p	-1.76	1.56	2.67	-3.74	-0.18	-0.63	-0.35	-0.74	1.67
hsa-miR-31-5p	5.04	4.95	4.81	1.97	7.37	6.84	5.16	0.42	1.77
hsa-miR-32-5p	2.57	5.75	6.22	2.78	6.29	4.32	4.65	0.42	0.78
hsa-miR-330-3p	7.31	9.48	10.27	4.79	9.08	7.32	8.04	0.96	0.42
hsa-miR-331-3p	2.19	3.73	4.11	3.27	2.54	2.82	3.11	0.29	0.46
hsa-miR-34a-5p	3.32	5.30	6.56	2.38	4.57	4.39	4.42	0.96	-0.06
hsa-miR-34b-3p	9.33	7.36	10.20	7.05	9.52	–	8.69	4.17	4.36
hsa-miR-34c-5p	–	7.35	9.34	8.24	9.61	–	8.63	4.34	3.58
hsa-miR-361-5p	-0.49	3.59	4.08	-1.72	0.97	-0.04	1.07	1.31	1.30

APPROVED GALLEY PROOF

Table 3 continued. Delta cycle threshold (Δ Ct) values for 6 metastatic Wilms tumor (WT) samples (from 5 patients). Logarithmic fold change (\log_2 FC) values between groups are shown in the right.

miRNA	Patient 5	Patient 9 (left lung met.)	Patient 9 (right lung met.)	Patient 10	Patient 11	Patient 12	Mean	\log_2 FC (metastatic to control)	\log_2 FC (metastatic to primary)
hsa-miR-365a-3p	3.40	5.91	6.92	6.63	6.15	5.03	5.67	-0.82	-0.85
hsa-miR-374b-5p	-0.24	4.50	5.05	-1.81	2.86	1.28	1.94	1.40	1.44
hsa-miR-375-3p	5.32	5.68	8.50	3.19	3.36	3.61	4.94	4.20	4.73
hsa-miR-425-5p	1.20	4.95	5.21	1.63	5.16	1.77	3.32	-0.90	0.96
hsa-miR-449a	11.68	9.05	11.92	-	9.56	-	10.55	-0.85	2.32
hsa-miR-455-5p	6.11	8.70	9.95	3.36	6.38	5.39	6.65	-0.71	0.09
hsa-miR-494-3p	8.76	11.66	11.38	8.68	8.21	8.77	9.58	1.14	-1.49
hsa-miR-616-3p	11.32	-	-	9.64	9.78	-	10.25	2.63	3.69
hsa-miR-7-5p	5.17	9.56	9.33	8.21	9.25	6.05	7.93	1.59	1.31
hsa-miR-9-3p	7.94	-	15.16	10.59	4.98	-	9.67	0.71	2.57
hsa-miR-92a-3p	-4.00	0.19	-0.19	-3.12	-1.54	-3.68	-2.05	1.45	1.10
hsa-miR-93-5p	-2.35	2.94	1.95	-2.29	2.27	-1.1	0.24	2.86	1.88
hsa-miR-96-5p	2.18	8.34	8.05	6.28	6.21	2.92	5.66	3.90	2.12
hsa-miR-99a-5p	1.13	3.07	5.41	-0.02	0.32	-1.42	1.42	-1.06	-0.60
hsa-miR-99b-5p	-1.49	2.20	2.58	-3.24	2.24	-0.6	0.28	1.36	1.16

Table 4. Delta cycle threshold (Δ Ct) values for 10 control samples.

miRNA	C1	C2	C3	C4	C5	C6	C7	C8	C9	C10	Mean
hsa-let-7a-5p	-1.32	-1.73	-0.95	-4.90	-1.95	-1.59	0.79	6.04	-0.92	-3.00	-0.95
hsa-let-7b-5p	-0.61	-1.19	-0.75	-4.13	-0.95	-1.28	0.99	1.91	-0.44	-1.80	-0.82
hsa-let-7c-5p	-0.09	-0.33	-0.02	-3.25	-0.35	-0.48	2.05	7.58	0.48	-1.74	0.39
hsa-let-7f-5p	0.86	1.33	1.89	-2.51	0.13	0.75	4.13	8.51	1.84	-1.30	1.56
hsa-miR-100-5p	1.51	1.80	2.46	-1.50	0.41	-0.91	4.38	5.4	1.28	0.74	1.56
hsa-miR-101-3p	2.57	3.66	4.59	-0.59	1.33	2.63	6.04	6.78	4.23	0.44	3.17
hsa-miR-106b-5p	2.90	3.26	4.78	1.31	2.28	2.65	6.78	8.24	4.28	1.69	3.82
hsa-miR-125a-5p	-1.70	-0.88	-0.79	-3.47	-2.02	-3.82	1.06	1.37	-2.43	-1.44	-1.41
hsa-miR-125b-5p	-2.47	-2.02	-1.23	-4.08	-2.71	-4.26	0.14	-0.05	-2.33	-2.70	-2.17
hsa-miR-126-3p	-1.28	-0.08	1.10	-4.35	-1.64	-1.74	2.89	5.36	0.28	-2.39	-0.18
hsa-miR-126-5p	2.62	4.64	4.45	-0.76	2.73	2.34	7.08	8.32	4.47	1.96	3.78
hsa-miR-128-3p	6.47	7.68	7.63	4.72	6.18	5.32	9.66	14.21	6.04	4.78	7.27
hsa-miR-133a-3p	3.64	4.08	4.92	3.88	5.39	2.97	7.61	13.02	4.77	4.18	5.45
hsa-miR-135a-5p	4.47	4.72	3.41	-0.97	2.75	1.55	5.61	5.79	3.84	1.42	3.26

APPROVED GALLEY PROOF

Table 4 continued. Delta cycle threshold (Δ Ct) values for 10 control samples.

miRNA	C1	C2	C3	C4	C5	C6	C7	C8	C9	C10	Mean
hsa-miR-135b-5p	6.20	4.67	5.99	2.97	5.34	4.40	8.86	9.71	5.78	5.54	5.95
hsa-miR-141-3p	2.69	3.05	3.88	-0.53	1.34	0.62	6.25	10.57	2.47	1.01	3.13
hsa-miR-143-3p	-0.47	-0.49	1.29	-1.78	-0.69	-0.66	4.14	6.53	1.18	-1.39	0.77
hsa-miR-145-5p	-2.86	-3.08	-1.96	-3.67	-2.47	-3.41	0.73	2.95	-2.10	-2.84	-1.87
hsa-miR-146a-5p	4.56	4.32	4.75	0.98	3.56	2.94	7.05	9.95	4.85	2.61	4.56
hsa-miR-146b-5p	3.20	3.61	5.43	0.71	2.68	3.28	6.85	7.05	3.94	2.34	3.91
hsa-miR-148a-3p	2.76	4.59	4.56	0.92	1.70	2.99	6.78	8.38	4.30	1.28	3.83
hsa-miR-15a-5p	2.60	3.20	3.64	0.28	1.74	2.23	5.99	6.22	3.69	0.36	2.99
hsa-miR-15b-5p	4.09	5.27	5.61	2.48	3.20	5.37	8.19	8.35	6.59	2.64	5.18
hsa-miR-16-5p	-0.51	0.10	0.98	-3.68	-1.58	-0.75	3.22	3.37	0.89	-2.35	-0.03
hsa-miR-17-5p	1.62	2.98	3.96	-0.16	1.17	2.47	6.27	6.29	4.14	0.78	2.95
hsa-miR-17-3p	6.47	7.21	8.32	4.33	6.48	5.40	10.59	11.59	7.16	5.29	7.28
hsa-miR-181a-5p	0.77	1.21	1.85	-1.90	0.37	-0.79	3.91	3.98	1.32	0.36	1.11
hsa-miR-181b-5p	3.76	3.35	3.61	0.58	2.99	2.25	5.33	5.53	3.69	2.75	3.38
hsa-miR-182-5p	7.89	8.18	10.28	5.70	7.26	7.12	11.79	14.7	8.75	5.86	8.75
hsa-miR-183-5p	8.84	7.88	9.55	5.87	8.32	7.51	11.83	16	8.72	6.88	9.14
hsa-miR-184	8.71	11.15	6.53	4.29	5.42	5.20	9.70	13.36	7.84	5.80	7.80
hsa-miR-194-5p	1.20	2.57	1.72	-3.71	-1.02	-0.27	3.18	6.35	1.11	-1.85	0.93
hsa-miR-195-5p	2.59	2.63	4.12	-0.22	1.62	2.69	6.52	5.3	4.86	1.73	3.18
hsa-miR-196a-5p	4.06	3.54	3.81	-0.72	2.69	2.16	6.59	6.92	4.28	2.15	3.55
hsa-miR-19b-3p	-0.04	1.67	3.30	-1.30	-0.92	0.57	4.65	4.63	1.88	-1.23	1.32
hsa-miR-200b-3p	1.09	1.37	2.21	-2.81	0.11	-1.01	4.06	7.82	0.50	-0.68	1.27
hsa-miR-200c-3p	0.57	1.07	1.31	-2.54	0.36	-1.76	3.30	7.51	-0.23	0.17	0.98
hsa-miR-203a-3p	5.93	7.21	7.38	3.06	4.79	4.45	9.94	13.39	6.43	5.23	6.78
hsa-miR-205-5p	8.63	8.11	9.70	9.12	9.38	2.72	10.89	14.51	4.24	10.36	8.77
hsa-miR-20a-5p	0.74	1.80	2.69	-1.84	0.22	0.75	4.89	4.78	2.30	-0.30	1.60
hsa-miR-20b-5p	7.51	11.66	10.35	6.63	7.68	8.70	13.59	14.35	10.47	7.80	9.87
hsa-miR-21-5p	-0.21	-2.59	0.70	-3.85	-1.05	-1.14	3.09	5.22	-0.39	-2.03	-0.22
hsa-miR-218-5p	5.62	5.87	7.14	1.23	4.52	4.13	8.47	12.17	5.46	3.28	5.79
hsa-miR-22-3p	1.79	1.34	2.12	-0.98	0.62	-0.61	4.01	9.69	0.83	-0.20	1.86
hsa-miR-221-3p	3.17	3.34	3.84	0.68	3.08	1.26	6.72	9.13	2.75	1.54	3.55
hsa-miR-222-3p	2.33	2.70	3.40	0.12	2.31	0.43	5.67	8.43	2.38	1.65	2.94
hsa-miR-223-3p	2.84	2.93	3.75	0.92	1.44	3.15	7.07	7.26	4.57	1.17	3.51
hsa-miR-224-5p	7.40	7.90	9.16	5.56	7.63	7.25	12.87	12.57	9.07	6.36	8.58
hsa-miR-23b-3p	-0.98	-0.52	0.32	-3.94	-1.77	-1.22	2.69	4.15	0.25	-1.52	-0.25

APPROVED GALLEY PROOF

Table 4 continued. Delta cycle threshold (Δ Ct) values for 10 control samples.

miRNA	C1	C2	C3	C4	C5	C6	C7	C8	C9	C10	Mean
hsa-miR-24-3p	-0.93	-0.31	1.27	-2.91	-1.46	-0.88	3.48	6.36	0.79	-1.54	0.39
hsa-miR-25-3p	2.83	2.68	3.66	-1.12	2.31	0.41	6.29	6.73	2.58	1.37	2.77
hsa-miR-26a-5p	-1.42	0.29	0.89	-4.28	-1.86	-0.97	3.38	2.12	0.64	-1.46	-0.27
hsa-miR-26b-5p	0.68	2.49	2.80	-2.55	0.35	1.46	5.29	7.38	3.04	-0.32	2.06
hsa-miR-27a-3p	0.47	1.24	1.97	-2.47	-0.28	-0.15	4.30	5.47	1.69	-0.18	1.21
hsa-miR-27b-3p	0.20	0.44	1.36	-3.57	-0.91	-1.09	3.58	5.54	0.81	-1.06	0.53
hsa-miR-296-5p	5.05	6.18	6.52	6.63	6.55	4.59	7.95	6.66	5.12	5.90	6.11
hsa-miR-29b-3p	4.24	4.18	3.33	1.01	3.48	1.58	7.38	7.18	2.82	3.87	3.91
hsa-miR-30c-5p	-1.82	-0.21	-0.16	-4.96	-3.24	-2.40	2.31	3.38	-0.91	-2.88	-1.09
hsa-miR-31-5p	5.72	6.06	5.92	4.35	4.85	3.86	8.00	–	5.49	5.96	5.58
hsa-miR-32-5p	5.31	4.87	5.60	2.03	4.54	3.86	7.03	9.06	4.93	3.49	5.07
hsa-miR-330-3p	8.00	8.31	9.86	7.55	8.65	7.58	11.12	11.82	7.87	9.25	9.00
hsa-miR-331-3p	2.96	3.07	3.55	3.22	3.31	0.98	4.77	6.41	2.17	3.57	3.40
hsa-miR-34a-5p	6.33	4.10	5.18	4.59	3.93	4.17	8.20	7.43	5.83	4.08	5.38
hsa-miR-34b-3p	10.90	–	14.56	10.19	13.47	11.22	16.86	–	–	–	12.87
hsa-miR-34c-5p	12.88	12.57	12.66	–	12.41	12.56	14.96	–	13.08	12.70	12.98
hsa-miR-361-5p	1.99	2.47	3.15	-0.41	1.70	1.13	4.82	5.08	2.39	1.48	2.38
hsa-miR-365a-3p	3.92	4.53	4.39	3.62	3.27	2.62	5.69	12.81	3.55	4.09	4.85
hsa-miR-374b-5p	2.58	3.27	4.37	-0.68	1.76	2.43	6.47	6.61	4.01	2.59	3.34
hsa-miR-375-3p	11.39	7.00	9.40	6.95	9.73	7.42	12.98	13.01	8.73	4.85	9.15
hsa-miR-425-5p	4.27	5.13	5.54	-22.79	3.57	2.71	7.94	8.98	4.42	4.44	2.42
hsa-miR-449a	15.61	11.71	14.66	-22.90	12.82	10.34	17.82	–	13.31	13.97	9.70
hsa-miR-455-5p	5.52	5.39	5.99	–	4.53	3.39	8.80	9.42	5.72	4.73	5.94
hsa-miR-494-3p	8.03	9.33	11.38	–	8.71	8.44	14.12	16.84	8.97	10.61	10.71
hsa-miR-616-3p	12.86	12.80	13.05	–	15.40	10.98	–	–	–	12.19	12.88
hsa-miR-7-5p	9.14	9.53	10.20	5.52	7.82	7.86	13.59	12.69	9.55	9.31	9.52
hsa-miR-9-3p	10.52	11.94	10.22	7.68	7.66	6.82	14.22	–	9.91	14.43	10.38
hsa-miR-92a-3p	-0.42	-0.07	-0.05	-2.70	-0.66	-2.06	1.51	0.44	-1.31	-0.76	-0.61
hsa-miR-93-5p	2.58	2.88	3.81	0.53	2.04	1.43	5.85	6.71	3.13	2.01	3.10
hsa-miR-96-5p	8.69	7.95	9.67	7.07	8.48	9.09	11.06	15.51	9.41	8.67	9.56
hsa-miR-99a-5p	0.06	1.11	1.14	-2.98	-0.73	-2.15	3.44	3.88	-0.19	-0.05	0.35
hsa-miR-99b-5p	1.25	1.90	2.43	-0.61	1.26	-0.79	3.97	4.36	0.45	2.17	1.64

APPROVED GALLEY PROOF

Table 5. Comparison of sample-level (n=6 metastatic lesions) and patient-level (n=5; one metastasis per patient, excluding the second lesion from patient 9) analyses of miRNA deregulation across 81 miRNAs.

miRNA	6 Samples			5 Samples		
	t test, control vs metastasis	t test, primary vs metastasis	Kruskal-Wallis test	t test, control vs metastasis	t test, primary vs metastasis	Kruskal-Wallis test
hsa-let-7a-5p	0.9821	0.9486	0.7817	0.6391	0.3424	0.6214
hsa-let-7b-5p	0.5450	0.7792	0.8445	0.9174	0.5922	0.7745
hsa-let-7c-5p	0.7713	0.9808	0.8386	0.4730	0.3244	0.5207
hsa-let-7f-5p	0.7961	0.3545	0.3713	0.4513	0.0630	0.1553
hsa-miR-100-5p	0.8817	0.7013	0.9691	0.6529	0.6471	0.9196
hsa-miR-101-3p	0.8659	0.1773	0.3364	0.7780	0.0589	0.1708
hsa-miR-106b-5p	0.0360	0.1539	0.1286	0.0323	0.1181	0.1060
hsa-miR-125a-5p	0.6865	0.3177	0.5355	0.3371	0.1038	0.2767
hsa-miR-125b-5p	0.5152	0.4252	0.8603	0.9162	0.9740	0.9972
hsa-miR-126-3p	0.6272	0.0071	0.0312	0.3414	0.0003	0.0086
hsa-miR-126-5p	0.3758	0.0501	0.1346	0.1444	0.0086	0.0345
hsa-miR-128-3p	0.2258	0.9441	0.3497	0.2150	0.8083	0.2741
hsa-miR-133a-3p	0.8240	0.1444	0.2633	0.7895	0.3010	0.4344
hsa-miR-135a-5p	0.3228	0.0605	0.1346	0.1822	0.0400	0.0783
hsa-miR-135b-5p	0.0041	0.0502	0.0234	0.0034	0.0440	0.0308
hsa-miR-141-3p	0.5324	0.0257	0.0063	0.7780	0.0150	0.0058
hsa-miR-143-3p	0.4636	0.6456	0.1625	0.7674	0.2190	0.1394
hsa-miR-145-5p	0.6262	0.5159	0.1920	0.9225	0.1255	0.1430
hsa-miR-146a-5p	0.5783	0.0587	0.1525	0.3605	0.0096	0.0671
hsa-miR-146b-5p	0.0744	0.2044	0.3753	0.0286	0.0766	0.1720
hsa-miR-148a-3p	0.8007	0.4455	0.2792	0.9457	0.2503	0.1872
hsa-miR-15a-5p	0.5622	0.7007	0.8750	0.3313	0.3149	0.5775
hsa-miR-15b-5p	0.0863	0.2293	0.1974	0.0469	0.1127	0.1042
hsa-miR-16-5p	0.2226	0.2203	0.4735	0.0950	0.0608	0.1635
hsa-miR-17-5p	0.0638	0.1068	0.1400	0.0680	0.1068	0.1333
hsa-miR-17-3p	0.0163	0.0188	0.0322	0.0129	0.0127	0.0247
hsa-miR-181a-5p	0.1457	0.4685	0.4372	0.0771	0.2804	0.2623
hsa-miR-181b-5p	0.0456	0.4427	0.2099	0.0178	0.2526	0.0974
hsa-miR-182-5p	0.0116	0.1395	0.0449	0.0083	0.0863	0.0393
hsa-miR-183-5p	0.0075	0.1240	0.0218	0.0046	0.0694	0.0128
hsa-miR-184	0.2439	0.0901	0.0157	0.2439	0.0901	0.0157
hsa-miR-194-5p	0.0267	0.1342	0.0012	0.0674	0.0748	0.0013

APPROVED GALLEY PROOF

Table 5 continued. Comparison of sample-level (n=6 metastatic lesions) and patient-level (n=5; one metastasis per patient, excluding the second lesion from patient 9) analyses of miRNA deregulation across 81 miRNAs.

miRNA	6 Samples			5 Samples		
	t test, control vs metastasis	t test, primary vs metastasis	Kruskal-Wallis test	t test, control vs metastasis	t test, primary vs metastasis	Kruskal-Wallis test
hsa-miR-195-5p	0.9394	0.1259	0.1769	0.6123	0.0421	0.1040
hsa-miR-196a-5p	0.0875	0.2498	0.4372	0.0492	0.1705	0.3219
hsa-miR-19b-3p	0.2730	0.0935	0.3525	0.1885	0.0617	0.2721
hsa-miR-200b-3p	0.0568	0.3516	0.0060	0.1452	0.1376	0.0050
hsa-miR-200c-3p	0.6787	0.0154	0.0062	0.9629	0.0052	0.0032
hsa-miR-203a-3p	0.8774	0.0007	0.0030	0.8105	0.0002	0.0028
hsa-miR-205-5p	0.2804	0.9958	0.1370	0.2659	0.8334	0.1330
hsa-miR-20a-5p	0.1055	0.1443	0.2855	0.0937	0.1251	0.2363
hsa-miR-20b-5p	0.8524	0.5248	0.5238	0.8470	0.5834	0.5668
hsa-miR-21-5p	0.5089	0.7318	0.7721	0.2501	0.2247	0.4250
hsa-miR-218-5p	0.0474	0.0695	0.1438	0.0360	0.0418	0.1200
hsa-miR-22-3p	0.2657	0.3870	0.0445	0.4083	0.7565	0.0647
hsa-miR-221-3p	0.2087	0.1099	0.2994	0.1379	0.0486	0.1453
hsa-miR-222-3p	0.4531	0.3095	0.5725	0.2487	0.0804	0.2352
hsa-miR-223-3p	0.1989	0.1282	0.2462	0.0753	0.0179	0.0548
hsa-miR-224-5p	0.1659	0.1445	0.2840	0.0647	0.0148	0.0683
hsa-miR-23b-3p	0.3327	0.1950	0.5656	0.1686	0.0790	0.3178
hsa-miR-24-3p	0.3970	0.1181	0.4612	0.2371	0.0321	0.2252
hsa-miR-25-3p	0.0111	0.0698	0.0679	0.0045	0.0306	0.0433
hsa-miR-26a-5p	0.8402	0.3175	0.5858	0.4743	0.0977	0.3037
hsa-miR-26b-5p	0.7667	0.3283	0.5580	0.4786	0.1069	0.2790
hsa-miR-27a-3p	0.4691	0.1480	0.3673	0.2171	0.0300	0.1462
hsa-miR-27b-3p	0.4658	0.1289	0.4139	0.2499	0.0354	0.1920
hsa-miR-296-5p	0.0705	0.1355	0.3364	0.0564	0.1042	0.3861
hsa-miR-29b-3p	0.1174	0.4827	0.0539	0.2012	0.3620	0.0530
hsa-miR-30c-5p	0.5680	0.1423	0.1041	0.9167	0.0536	0.0700
hsa-miR-31-5p	0.6091	0.0316	0.0540	0.6992	0.0571	0.0683
hsa-miR-3163	-	-	-	-	-	-
hsa-miR-32-5p	0.6692	0.3918	0.5301	0.4864	0.2643	0.4430
hsa-miR-330-3p	0.2902	0.5821	0.6228	0.1369	0.2592	0.3303
hsa-miR-331-3p	0.6553	0.2815	0.6057	0.4844	0.1396	0.3547
hsa-miR-34a-5p	0.2342	0.9369	0.4608	0.0960	0.6007	0.3054

APPROVED GALLEY PROOF

Table 5 continued. Comparison of sample-level (n=6 metastatic lesions) and patient-level (n=5; one metastasis per patient, excluding the second lesion from patient 9) analyses of miRNA deregulation across 81 miRNAs.

miRNA	6 Samples			5 Samples		
	t test, control vs metastasis	t test, primary vs metastasis	Kruskal-Wallis test	t test, control vs metastasis	t test, primary vs metastasis	Kruskal-Wallis test
hsa-miR-34b-3p	0.0102	0.0001	0.0061	0.0119	0.0001	0.0106
hsa-miR-34c-5p	< 0.0001	0.0043	0.0100	< 0.0001	0.0080	0.0255
hsa-miR-361-5p	0.2055	0.2077	0.4402	0.0690	0.0691	0.1626
hsa-miR-365a-3p	0.5272	0.1420	0.0969	0.6845	0.3058	0.1739
hsa-miR-3662	–	–	–	–	–	–
hsa-miR-3666	–	–	–	–	–	–
hsa-miR-374b-5p	0.2724	0.2463	0.5964	0.1286	0.1100	0.2790
hsa-miR-375	0.0056	0.0009	0.0083	0.0021	0.0002	0.0047
hsa-miR-425-5p	0.8164	0.2615	0.6033	0.9025	0.1373	0.3966
hsa-miR-449a	0.8967	0.0412	0.1514	0.9589	0.0288	0.1421
hsa-miR-455-5p	0.5397	0.9221	0.5392	0.9679	0.4123	0.5256
hsa-miR-494-3p	0.4070	0.0868	0.0754	0.3146	0.1968	0.0888
hsa-miR-616-3p	0.0258	0.0115	0.0280	0.0258	0.0115	0.0280
hsa-miR-7-5p	0.1789	0.2383	0.3298	0.1477	0.1889	0.2842
hsa-miR-9-3p	0.7241	0.2154	0.3880	0.1995	0.0334	0.1274
hsa-miR-92a-3p	0.0741	0.2285	0.3110	0.0333	0.1304	0.1838
hsa-miR-93-5p	0.0200	0.1286	0.1024	0.0166	0.0988	0.1114
hsa-miR-96-5p	0.0077	0.1338	0.0181	0.0057	0.0886	0.0128
hsa-miR-99a-5p	0.3809	0.5352	0.6083	0.8160	0.7964	0.7141
hsa-miR-99b-5p	0.2083	0.2742	0.7300	0.1121	0.1482	0.4338
Median p value	0.3228	0.1950	0.2840	0.2150	0.0988	0.1462

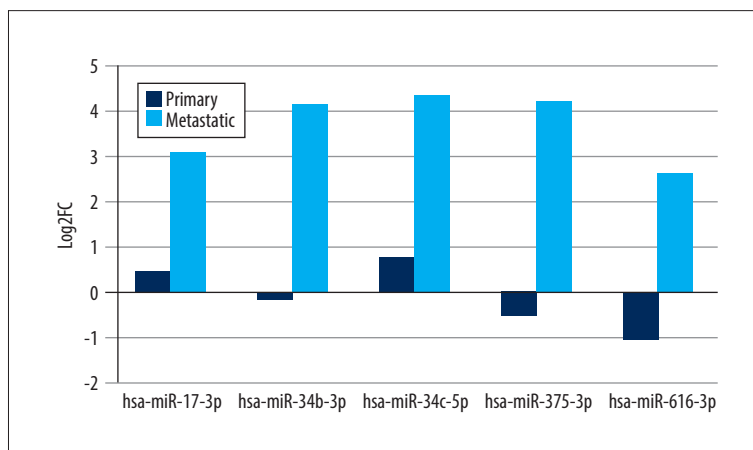


Figure 1. Expression differences of selected miRNAs in primary and metastatic tumors compared with control samples (in log₂FC).

APPROVED GALLEY PROOF

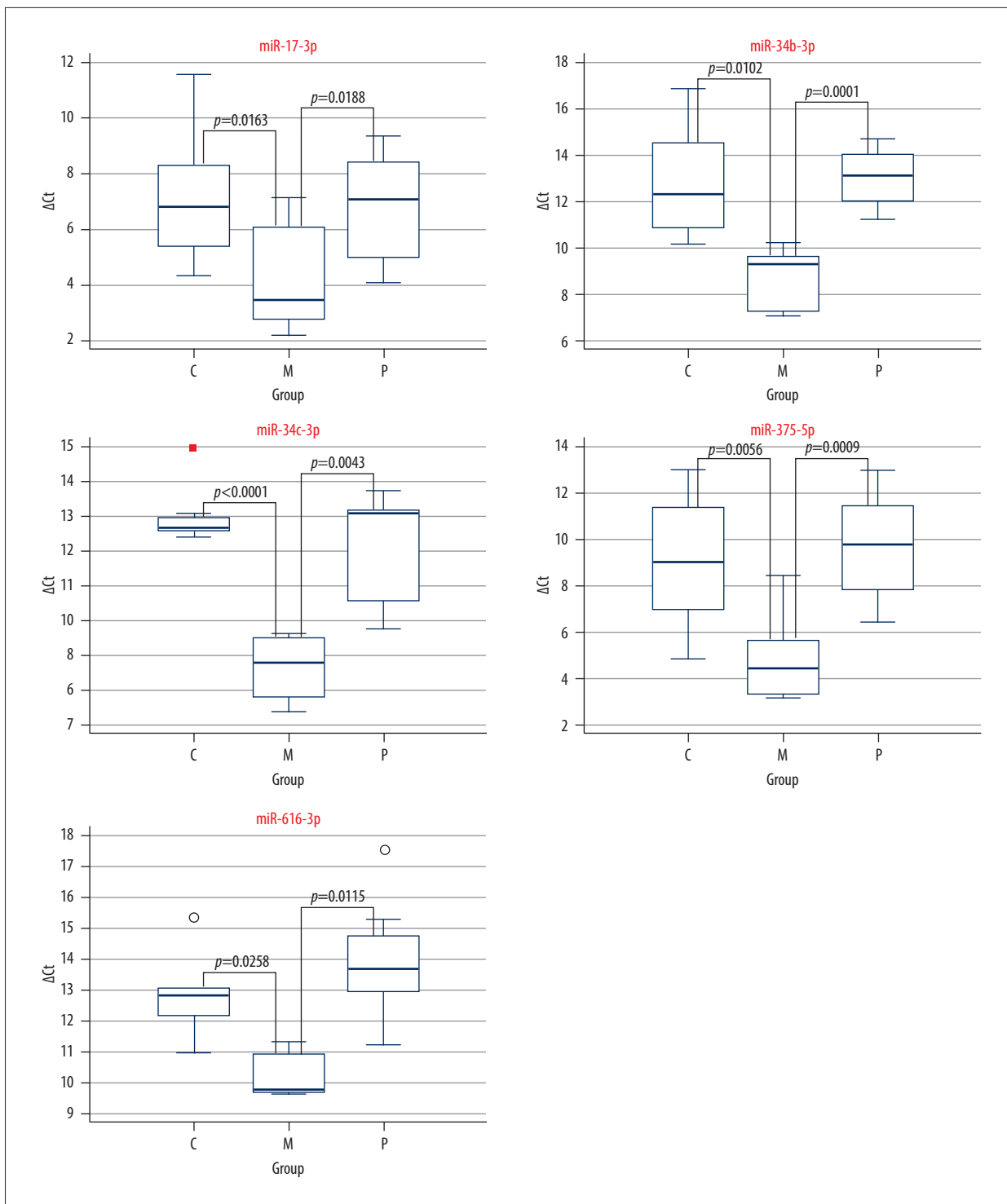


Figure 2. Box-and-whiskers plots of miRNAs displaying $P \leq 0.05$ in the Kruskal-Wallis test and t tests for independent samples. "C" indicates control group, "M" metastatic, and "P" primary tumor group.

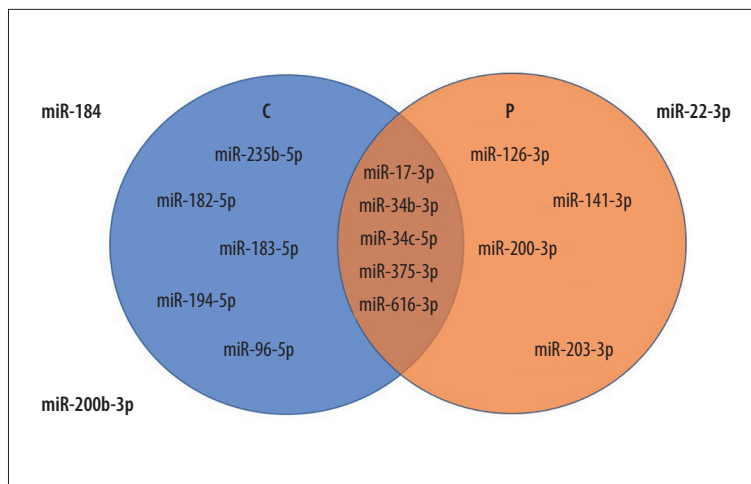


Figure 3. miRNAs that displayed $P \leq 0.05$ in the Kruskal-Wallis test. Outside the Venn diagram: $P \leq 0.05$ in the Kruskal-Wallis test only; C (control vs metastasis) and P (primary vs metastasis): $P \leq 0.05$ in the corresponding t test for independent samples in addition to the Kruskal-Wallis test.

(hsa-miR-3163, hsa-miR-3662, and hsa-miR-3666) were excluded from further analysis due to a lack of amplification in any of the metastatic samples, as well as in most healthy tissue and primary tumor samples. Five miRNAs (miR-17-3p, miR-34b-3p, miR-34c-5p, miR-375-3p, and miR-616-3p) produced low P values both in the 2 t tests (ranging between $P < 0.0001$ and 0.0258) and in the Kruskal-Wallis test (between $P = 0.0061$ and $P = 0.0322$) with all 6 metastatic samples included (Table 5). Interestingly, expression levels of all 5 miRNAs were higher in metastatic samples than in primary WTs and control samples (Table 3; Figures 1, 2). The identified miRNA deregulations (Figure 3) are explored further in the Discussion.

Network Analysis

The results of our network analyses are shown in Figure 4. We identified 43 genes that are regulated by at least 2 of the studied miRNAs. Among these, polypeptide N-acetylgalactosaminyltransferase 7 (GALNT7), methylenetetrahydrofolate dehydrogenase (NADP⁺-dependent) 1 (MTHFD1), Scm-related gene containing four Mbt domains 2 (SFMBT2) and cyclin-dependent kinase 4 (CDK4) seem the most relevant based on degree and betweenness values. On the same basis, the role of miR-34b-3p seems to be central within the network.

We note that our network analysis was based on predicted interactions. However, GALNT7 has been experimentally validated as a target of miR-17-3p and miR-34c-5p [17,18]. The interaction of CDK4 with miR-34b-3p and miR-34c-5p has also been validated [19].

A functional gene enrichment analysis was also performed based on identified miRNA-mRNA interactions. According to the Reactome database, these miRNAs regulate the expression of several proteins involved in the regulation of cell death by influencing TP53 and NOTCH signaling as well as the cell cycle. KEGG pathway analysis showed strong enrichment in

“Pathways in cancer” and in specific cancer types, including genitourinary neoplasms (Figure 4).

Inpatient Variability Between Primary and Metastatic WT Samples

In cases in which multiple metastatic or primary samples were available from the same patient, individual miRNA profiles were arranged from left to right in order of increasing similarity of expression (Figure 5). The 2 metastatic samples from patient 9 showed remarkably similar deregulation patterns, with some miRNAs differing in expression levels but maintaining the same direction of change. Primary samples of different histological types in patient 12 displayed greater variation, both between each other and in comparison with the metastatic sample.

To assess whether the 10 primary tumor samples can be treated as independent observations or whether same-patient origin should be accounted for, we performed a permutation analysis based on pairwise differences in ΔCt values. For each miRNA, we computed the absolute difference in ΔCt for all possible pairs of samples. The permutation P value was defined as the probability that a randomly selected pair would exhibit an absolute ΔCt difference less than or equal to that observed between the 2 primary tumor samples from patient 12 (all permutation P values are reported in Table 2). The median permutation P value across miRNAs was 0.47, indicating that the 2 samples from patient 12 were not more similar to each other than expected by chance relative to other sample pairs.

The 2 metastatic samples from patient 9 exhibited highly concordant miRNA deregulation patterns across the panel, making additional similarity testing uninformative. To address potential intra-patient correlation, we therefore repeated all statistical analyses using a patient-level dataset in which each patient contributed a single metastatic lesion ($n = 5$), omitting

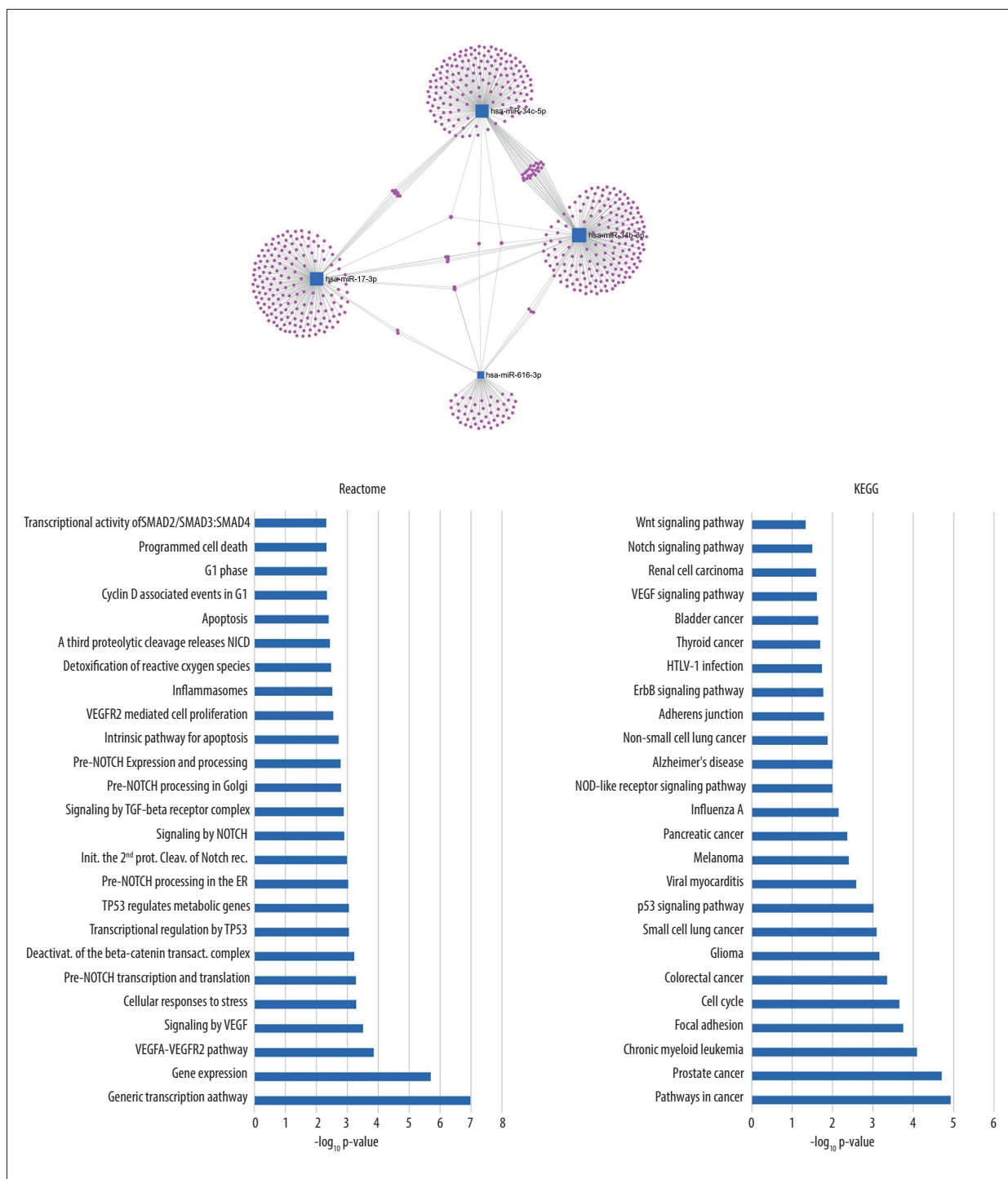
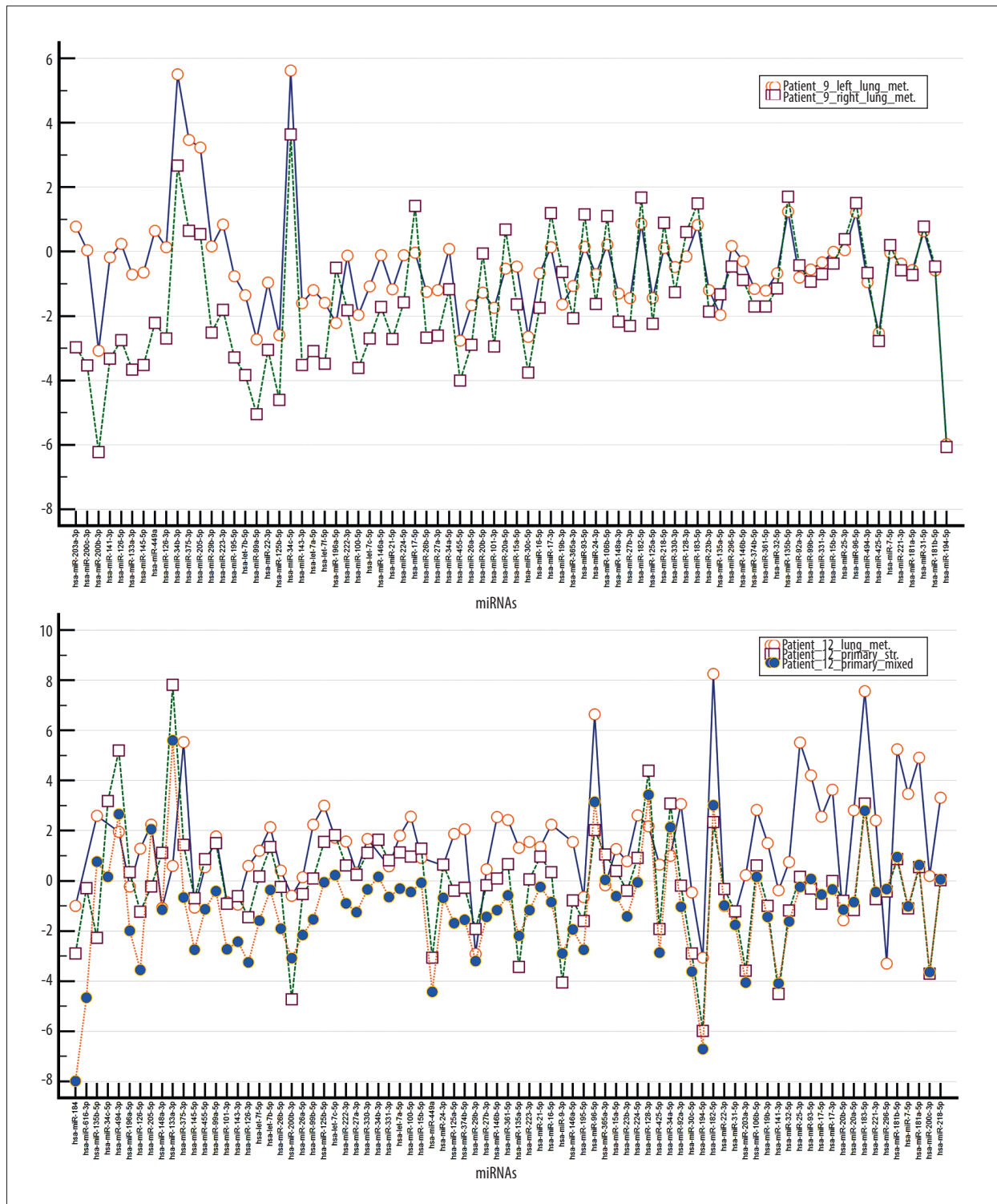


Figure 4. Top: Network analysis results for miR-17-3p, miR-34b-3p, miR-616-3p, and miR-34c-5p (from miRNet). miR-375-3p is not included due to a lack of known interacting partners. Blue squares represent the studied miRNAs, while pink dots correspond to interacting proteins. **Bottom:** Functional enrichment of the miRNA-mRNA interaction network using Reactome (left) and KEGG (right) via miRNet; the top 25 pathways are shown.



APPROVED GALLEY PROOF

Figure 5. Comparing log₂FC values of all miRNAs in the left and right lung metastasis found in patient 9 (**top**) and the primary stromal, primary mixed, and metastatic sample of patient 12 (**bottom**) using multiple line graphs. In the case of patient 12 with 3 samples compared, the similarity between the 2 primary samples was the basis of alignment.

the chronologically second metastatic sample from patient 9. The direction and overall pattern of miRNA deregulations were unchanged, and median *P* values across the 81 miRNAs were lower in the patient-level analysis than in the sample-level analysis (Table 5). These findings indicate that the observed differences are not driven by the inclusion of 2 metastatic lesions from a single patient. Given that the sample-level analysis (*n*=6 metastatic lesions) yielded higher *P* values despite the larger sample size, it was considered the more statistically conservative approach and was retained as the primary analysis underlying the reported findings, while patient-level results are presented in parallel for completeness.

Discussion

WT Metastases and Their miRNA Signatures

At diagnosis, approximately 17% of patients have indications of hematogenous metastasis, and most of them involve the lungs. Less typical locations include liver and bones. High-risk tumors and relapses of metastatic disease have a poorer prognosis [20]. With a combination of chemotherapy (adjuvant and/or neoadjuvant), surgery, and radiation therapy, an overall survival exceeding 90% has been achieved for localized WT. Overall survival for metastasized WT is about 75%, while in the case of recurrence, it is 50% [21]. The molecular background distinguishing primary and metastatic tumors could reveal deregulated processes that may help clinicians identify biologically aggressive cases even before a metastasis develops. A well-established miRNA profile may prove to be an important piece to that puzzle.

Expression of miRNAs has already been reported in progressing and metastatic WT, but evidence is scarce. Pérez-Linares et al found differential expressions for several miRNAs applying TaqMan low-density array followed by validation cohort trials (RT-qPCR and in situ hybridization). miR-29a had low expression in both FHWT (favorable histology Wilms' tumor) and metastatic disease. Expression differences between the metastatic and control groups were more significant. They also reported a lower expression of miR-200b-3p in metastasis compared with the control group [11]. In the present research, this miRNA was found to be similarly expressed in metastatic and primary tumors (Tables 2, 3), but results reported by Pérez-Linares et al may be more informative given their larger sample size (*n*=21 metastatic samples compared with our *n*=6).

Zhang et al noted the downregulation of miR-203-5p in WT tissue [22]. We found the same alteration in our own dataset in primary but not in metastatic WTs (Tables 2-4). However, another group suggested a close correlation between miR-203-5p levels and the presence of lymphatic metastases, concluding

that miR-203a-5p may function as a tumor-suppressor in the development of WT [10].

Our Findings in Literature Context

Among the 81 miRNAs profiled in this study, several exhibited distinct expression differences between primary and metastatic samples (Tables 2, 3). In the following discussion, we focus on miRNAs with the strongest statistical support: miR-17-3p, miR-34b-3p, miR-34c-5p, and miR-375-3p. We also include miR-616-3p, which yielded low *P* values in parametric and nonparametric tests (Figure 3); however, interpretation is limited by the low number of successful amplifications, as explained below (Tables 2-4). As this study is cross-sectional in design, causal relationships with metastasis cannot be inferred, but observed expression differences may still serve as a basis for hypothesis generation.

The role of miR-17-3p in invasion, tumor proliferation, and metastasis was reported in several cancer types. Liu et al found an overexpression of miR-17-3p in WT tissues compared with healthy adult kidney samples [23]. miR-17-3p is a member of Oncomir-1, an oncogenic cluster of miRNAs. Kort et al profiled the expressions of several Oncomir-1 members (miR-17-3p was not included, but miR-17-5p was), and found them to be overexpressed in WT compared with other kidney tumor types [24]. miR-17 was also significantly deregulated in the blood samples of patients with WT before therapy compared with normal controls [25]. In prostate cancer development, the circSMARCA5-miR-181b-5p/miR-17-3p-tissue inhibitor of metalloproteinase 3 (TIMP3) axis is crucial. Both miRNAs may attenuate circSMARCA5 function, affecting tumor migration and invasion [26]. miR-17-3p may also promote tumor growth in prostate cancer by repressing TIMP3 [27]. In our dataset, consistent with findings in other cancer types, miR-17 appears to be highly expressed in metastatic WT (displaying a log₂FC value of 3.1 between metastatic and control, and 2.64 between metastatic and primary tumor samples in our study).

In the case of miR-34b-3p, minimal or no expression occurred in control and primary samples, while metastatic samples showed a moderate expression (log₂FC: 4.17 metastatic vs control; 4.36 metastatic vs primary). miR-34c-5p showed a similar pattern (log₂FC: 4.34 metastatic vs control; 3.58 metastatic vs primary). miR-34b-3p engages in the network of the TP53 tumor suppressor and may sabotage the p53-DAPK axis by dysregulating essential proteins such as BCL2 apoptosis regulator or cellular MYC [28]. Huang et al found it to be downregulated in the serum of patients with renal cell carcinoma, while upregulation was observed in the renal cell carcinoma tissue [28,29]. Still, the miR-34 family is predominantly recognized as a tumor suppressor in malignancies of the genitourinary system (and other tissues), with oncogenic roles barely reported [30].

Although our data are cross-sectional, the observed expression differences raise the possibility that such a role may exist in the context of WT metastases. In addition to miR-34b-3p and miR-34c-5p discussed above, miR-34a expression levels were also higher in our dataset. However, this pattern was observed similarly in primary and metastatic disease, and the corresponding *P* value (0.23) does not provide strong statistical support for the observation. Nevertheless, the consistency of our data across 3 different members of the miRNA family, all pointing toward the same interpretation, is intriguing. While miR-34 family members have rarely been studied in WT before, Liu et al investigated the expression of miR-34a-5p and, like us, reported an upregulation (with a fold change of 3.23 compared with adult normal kidney and 4.34 compared with fetal kidney samples) [23]. Similarly, Ludwig et al observed an increase in the expression of miR-34a (fold change: 5.47) and miR-34b (fold change: 2.26) in WT tissue [31]. In light of our findings within the context of existing literature, we propose that the miR-34 family may function differently in WT than in most other cancer types. We encourage further research to explore this possibility in greater depth.

In our sample pool, miR-375-3p showed a consistently higher expression in metastatic samples compared with control and primary tumor samples (\log_2 FC: 4.2 metastatic vs control; 4.73 metastatic vs primary). To our knowledge, no other authors have studied this miRNA in WT yet, but in colorectal cancer, its expression has been reported to both increase [32] and decrease [33] in association with metastasis. This dual role may be explained by the miRNA's ability to inhibit autophagy [34]. Autophagy is known to promote most cancers, but blocking it may play a paradoxical role in metastasis, facilitating the dissemination of tumor cells into large, advanced macrometastases [35]. In advanced cancer, an increase in miR-375 expression may also contribute to the tumor's escape from immune surveillance [32].

The most uncertain results were obtained with miR-616-3p due to overall high Ct values and expression being detectable in only 3 out of 6 metastatic samples (Tables 2-4). Acknowledging the limitations of interpretation, we tentatively suggest that its expression may be higher in metastasis than in both the control and primary samples (\log_2 FC: 2.63 metastatic vs control; 3.69 metastatic vs primary). The role of this miRNA has been reported in several tumor types but not in WT. An upregulation of miR-616-3p has been observed in prostatic and hepatocellular carcinoma. miR-616-3p overexpression was also observed in human gastric cancer, with a suggested role in

angiogenesis and epithelial-mesenchymal transition [36]. miR-616 acts as an oncogene in glioma, non-small cell lung cancer, and breast cancer. Promotion of migration, invasion, and proliferation in breast cancer by directly targeting TIMP2 has been demonstrated by functional in vitro experiments [37].

Conclusions

To gain a better understanding of WT pathogenesis and metastasis development, an analysis of miRNA deregulation may offer a relatively accessible key as miRNAs can be studied using FFPE samples (typically available in large numbers) and play important roles in suppressing gene expression. Such contributions may be integrated into the broader understanding of disease mechanisms.

In the context of limited available literature, our findings highlight a set of miRNAs that may be of interest in metastatic WT. These observations are exploratory and warrant further investigation to clarify their relevance and possible involvement in WT pathogenesis.

Institutional Review Board Statement

The study was conducted in accordance with the Declaration of Helsinki and approved by the Human Investigation Review Board, University of Szeged, Albert Szent-Györgyi Medical and Pharmaceutical Centre (protocol code: 188/2019-SZTE; date of approval: February 17, 2020) and by the Semmelweis University Regional and Institutional Committee of Science and Research Ethics (protocol code: SE RKEB 27/2020; date of approval: March 16, 2020).

Data Availability Statement

Additional data are available from the authors upon request.

Informed Consent Statement

Informed consent was obtained from all participants involved in the study.

Declaration of Figures' Authenticity

All figures submitted have been created by the authors who confirm that the images are original with no duplication and have not been previously published in whole or in part.

References:

- Ghafoor T, Bashir F, Ahmed S, Khalil S, Farah T. Predictors of treatment outcome of Wilms Tumour in low-income country; single centre experience from Pakistan. *J Pediatr Urol.* 2020;16(3): 375.e1-e7
- Neagu MC, David VL, Iacob ER, et al. Wilms' tumor: A review of clinical characteristics, treatment advances, and research opportunities. *Medicina (Kaunas).* 2025;61(3):491
- Phelps HM, Kaviany S, Borinstein SC, Lovvorn HN 3rd. Biological drivers of Wilms tumor prognosis and treatment. *Children.* 2018;5(11):145
- van den Heuvel-Eibrink MM, Hol JA, Pritchard-Jones K, et al. Position paper: Rationale for the treatment of Wilms tumour in the UMBRELLA SIOP-RTSG 2016 protocol. *Nat Rev Urol.* 2017;14(12):743-52
- Perotti D, Williams RD, Wegert J, et al. Hallmark discoveries in the biology of Wilms tumour. *Nat Rev Urol.* 2024;21(3): 158-80
- Dome JS, Perlman EJ, Graf N. Risk stratification for wilms tumor: Current approach and future directions. *Am Soc Clin Oncol Educ Book.* 2014;34(1):215-23
- Tagoe LG, Bonney NYA, Amoako E, et al. Unusual metastatic patterns of Wilms tumor: A case series. *Cureus.* 2024;16(2):e54640
- Shuai R, Li-Na S, Rui Z, et al. Serum exosomal hsa-let-7f-5p: A potential diagnostic biomarker for metastatic pancreatic cancer detection. *World J Gastroenterol.* 2025;31(26):109500
- O'Brien J, Hayder H, Zayed Y, Peng C. Overview of microRNA biogenesis, mechanisms of actions, and circulation. *Front Endocrinol.* 2018;9:402
- Bao J-W, Li W-J, Guo J-H, et al. MiRNA-203a-5p alleviates the malignant progression of Wilms' tumor via targeting JAG1. *Eur Rev Med Pharmacol Sci.* 2020;24(10):5329-35
- Pérez-Linares FJ, Pérezpeña-Diazconti M, García-Quintana J, et al. microRNA profiling in Wilms tumor: Identification of potential biomarkers. *Front Pediatr.* 2020;8:337
- Buglyó G, Magyar Z, Romicsné Görbe É, et al. Quantitative RT-PCR-based miRNA profiling of blastemal Wilms' tumors from formalin-fixed paraffin-embedded samples. *J Biotechnol.* 2019;298:11-15
- Buglyó G, Magyar Z, Romicsné Görbe É, et al. miRNA profiling of Hungarian regressive Wilms' tumor formalin-fixed paraffin-embedded (FFPE) samples by quantitative real-time polymerase chain reaction (RT-PCR). *Med Sci Monit.* 2021;27:e932731
- Li Q, Li M, Zheng K, et al. Detection of microRNA expression levels based on microarray analysis for classification of idiopathic pulmonary fibrosis. *Exp Ther Med.* 2020;20(4):3096-103
- Csók Á, Micsik T, Magyar Z, et al. Alterations of miRNA expression in diffuse hyperplastic perilar nephroblastomatosis: Mapping the way to understanding Wilms' tumor development and differential diagnosis. *Int J Mol Sci.* 2023;24(10):8793
- Jones W, Greytak S, Odeh H, et al. Deleterious effects of formalin-fixation and delays to fixation on RNA and miRNA-Seq profiles. *Sci Rep.* 2019;9(1):6980
- Shan SW, Fang L, Shatseva T, et al. Mature miR-17-5p and passenger miR-17-3p induce hepatocellular carcinoma by targeting PTEN, GalNT7 and vimentin in different signal pathways. *J Cell Sci.* 2013;126(6):1517-30
- Li W, Ma H, Sun J. MicroRNA 34a/c function as tumor suppressors in Hep 2 laryngeal carcinoma cells and may reduce GALNT7 expression. *Mol Med Rep.* 2014;9(4):1293-98
- Suzuki H, Yamamoto E, Nojima M, et al. Methylation-associated silencing of microRNA-34b/c in gastric cancer and its involvement in an epigenetic field defect. *Carcinogenesis.* 2010;31(12):2066-73
- Davidoff AM. Wilms tumor. *Adv Pediatr.* 2012;59(1):247-67
- Theilen T-M, Braun Y, Bochennek K, et al. Multidisciplinary treatment strategies for Wilms tumor: Recent advances, technical innovations and future directions. *Front Pediatr.* 2022;10:852185
- Zhang F, Zeng L, Cai Q, et al. Comprehensive analysis of a long noncoding RNA-associated competing endogenous RNA network in Wilms tumor. *Cancer Control.* 2020;27(2):1073274820936991
- Liu M, Roth A, Yu M, et al. The IGF2 intronic miR-483 selectively enhances transcription from IGF2 fetal promoters and enhances tumorigenesis. *Genes Dev.* 2013;27(23):2543-48
- Kort EJ, Farber L, Tretiakova M, et al. The E2F3-Oncomir-1 axis is activated in Wilms' tumor. *Cancer Res.* 2008;68(11):4034-38
- Schmitt J, Backes C, Nourkhami-Tutdibi N, et al. Treatment-independent miRNA signature in blood of Wilms tumor patients. *BMC Genomics.* 2012;13:379
- Xie X, Sun F-K, Huang X, et al. A circular RNA, circSMARCA5, inhibits prostate cancer proliferative, migrative, and invasive capabilities via the miR-181b-5p/miR-17-3p-TIMP3 axis. *Aging.* 2021;13(15):19908-19
- Yang X, Du WW, Li H, et al. Both mature miR-17-5p and passenger strand miR-17-3p target TIMP3 and induce prostate tumor growth and invasion. *Nucleic Acids Res.* 2013;41(21):9688-704
- Huang G, Li X, Chen Z, et al. A Three-microRNA panel in serum: Serving as a potential diagnostic biomarker for renal cell carcinoma. *Pathol Oncol Res.* 2020;26(4):2425-34
- Shiomi E, Sugai T, Ishida K, et al. Analysis of expression patterns of microRNAs that are closely associated with renal carcinogenesis. *Front Oncol.* 2019;9:431
- Fu J, Imani S, Wu M-Y, Wu R-C. microRNA-34 family in cancers: Role, mechanism, and therapeutic potential. *Cancers (Basel).* 2023;15(19):4723
- Ludwig N, Werner TV, Backes C, et al. Combining miRNA and mRNA expression profiles in Wilms tumor subtypes. *Int J Mol Sci.* 2016;17(4):475
- Meltzer S, Bjørnstrøm T, Lyckander LG, et al. Circulating exosomal miR-141-3p and miR-375 in metastatic progression of rectal cancer. *Transl Oncol.* 2019;12(8):1038-44
- Xu L, Wen T, Liu Z, et al. MicroRNA-375 suppresses human colorectal cancer metastasis by targeting Frizzled 8. *Oncotarget.* 2016;7(26):40644-56
- Chang Y, Yan W, He X, et al. miR-375 inhibits autophagy and reduces viability of hepatocellular carcinoma cells under hypoxic conditions. *Gastroenterology.* 2012;143(1):177-87.e8
- Marsh T, Tolani B, Debnath J. The pleiotropic functions of autophagy in metastasis. *J Cell Sci.* 2021;134(2):jcs247056
- Wu Z-H, Lin C, Liu C-C, et al. MiR-616-3p promotes angiogenesis and EMT in gastric cancer via the PTEN/AKT/mTOR pathway. *Biochem Biophys Res Commun.* 2018;501(4):1068-73
- Yuan C. miR-616 promotes breast cancer migration and invasion by targeting TIMP2 and regulating MMP signaling. *Oncol Lett.* 2019;18(3):2348-55